1 Introduction

Dynamical Mean-Field theory (DMFT) has proven to be a fantastic tool to study the Hubbard model and Mott-Hubbard transitions. Still, the nature of Mott-Hubbard transitions is complex as we get away from the most simple models. Notably, in the years 2003 to 2005, a controversy was sparked regarding the existence of Orbital-Selective Mott Transitions (OSMTs). Indeed, in many transition metal oxides, multiple bands typically cross the Fermi surface, notably the t_{2g} or e_g orbitals, and different bandwidths for different bands might give rise to multiple transition for each bands. This is the case for the cuprate $Ca_{2-x}Sr_xRuO_4$ which undergoes a Mott transition as x is increased from 0 [1].

The model considered in this paper will be the case of two bands, one narrow ($W = 2$) and one wide band ($W = 4$). The Hamiltonian used will be the Hubbard hamiltonian with interband coupling accounting for Hund's exchange :

$$\begin{aligned} H = &- \sum_{\langle i,j\rangle m\sigma} t_m \hat{c}^\dagger_{im\sigma}\hat{c}_{jm\sigma} \\ &+ U\sum_{im\sigma}\hat{n}_{im\uparrow}\hat{n}_{im\downarrow} + \sum_{i\sigma\sigma'}\left(U' - \delta_{\sigma\sigma'}J_z\right)\hat{n}_{i1\sigma}\hat{n}_{i2\sigma'} \\ &+ \frac{J_\perp}{2}\sum_{im\sigma}\hat{c}^\dagger_{im\sigma}\left(\hat{c}^\dagger_{i\bar{m}\bar{\sigma}}\hat{c}_{im\bar{\sigma}} + \hat{c}^\dagger_{im\bar{\sigma}}\hat{c}_{i\bar{m}\bar{\sigma}}\right)\hat{c}_{i\bar{m}\sigma} \end{aligned}$$

This model takes into account single-band Coulomb repulsion with the term in U, interband repulsion with $U' = U - 2J_z$ and Hund's exchange may be kept asymmetric (J_z model) or simplified with $J_z = J_{perp} = J$ if the system is invariant under spin rotation (J model). Sum indices denote sites (i, j), band ($m = 1, 2$) and spin ($\sigma = \uparrow, \downarrow$) with bars indicating the opposite state for the two states variables.

Initial results from Liebsch refuted the existence of OSMT for the J_z model using a DMFT method with Quantum Monte-Carlo (QMC) solver at finite temperature [2] [3]. However, multiple papers later contradicted Liebsch's results and found an OSMT, first Koga et al. using DMFT with exact diagonalisation (ED) at zero temperature and the full J model [4], arguing that $J \perp$ was necessary for OSMT observation [5], then Knecht et al. using DMFT with an improved QMC solver attempting to get rid of the sign problem at low temperature [6], using the same J_z model as Liebsch, and refuted both previous articles. Finally Arita and Held also found an OSMT using projective QMC (PQMC) to tackle the J model at zero temperature [7]. Liebsch has also published an answer to Knecht et al., comparing directly results from both articles [8].

2 Methods

Our goal in this paper is to use DMFT with a QMC solver to clarify the controversy and ensure the two-band Mott transition predictions is well understood and well described with current methods. To that end, we choose to study the full J model, which supposedly encompasses the full effects of correlation, and is also more interesting as it has only been studied at 0 temperature, contrary to the Jz model. In the Hamiltonian, t_m is set to 1 to set the energy scale. The parameters are chosen in accordance with previous papers on the matter, with the value of U variable and the ratios $J = U/4$ and $U' = U - 2J = U/2$ fixed ; additionally the two bands are set with bandwidths $W_1 = 2eV$ and $W_2 = 4eV$ in an elliptical density of states given by $\rho_i(\epsilon) = \frac{4}{\pi W_i}\sqrt{1 - 4\epsilon^2/W_i^2}$, and taken at half filling. Finally temperature is set to $\beta = \frac{1}{40}eV$, about room temperature.

In a Mott transition, the system undergoes a phase transition between a disordered phase for $U << t$, where the system is a conductor, and an ordered phase for $U >> t$, where the Coulomb repulsion prevents electron hopping and the system becomes an insulator. The difference between the two phases is striking when looking at the spectral function. In the insulating phase, all the spectral weight is contained in two lobes separated by a (Mott) gap. The non zero quasi-particle weight at zero frequency is a signature of the conductive phase: there are available states right above the last filled one and therefore no gap between the occupied and unoccupied states. Hence, to characterize the Mott transition, the parameter of choice is the quasi-particle weight at the Fermi energy, obtained from the self-energy:

$$Z_i = \frac{1}{1 - \dfrac{\partial}{\partial\omega}\Re(\Sigma_i)\Big|_{\omega=0}} \tag{1}$$

As the quasiparticle weight goes to zero, so does the spectral weight at $\omega = 0$, indicating an insulating state. For approximating the quasiparticle weight, we used a discrete approximation from the first Matsubara frequency. As the first Matsubara frequency is given by $\omega_0 = \pi/\beta$, we have

$$Z_i \approx \frac{1}{1 - \dfrac{\mathrm{Im}(\Sigma_i(i\omega_0))}{\omega_0}} = \frac{1}{1 - \dfrac{\beta}{\pi}\,\mathrm{Im}(\Sigma_i(i\omega_0))}. \tag{2}$$

To get the spectral function from the calculation of the Green's function on the Matsubara (imaginary) axis, we used the maximum entropy method for analytic continuation.

The in-house DMFT + QMC code used for this project has two main parameters to ensure convergence: the number of DMFT iterations n_{DMFT} and the time the QMC solver runs for each DMFT iteration, t_{QMC}. Other parameters worth mentioning are:

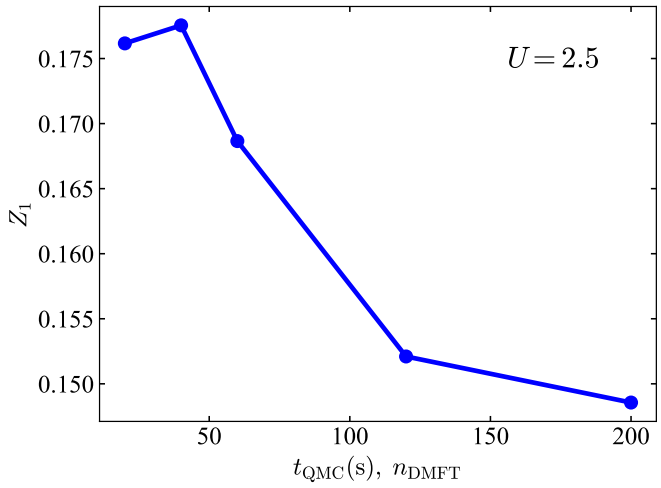

Figure 1: Convergence of the quasiparticle weight as a function of DMFT iterations and QMC time. The number of DMFT iterations and the number of seconds for the QMC time are the same and are varied from 20 to 200.

- The number of cores used for parallelisation, which is bound by the power of the computer used. We set this to 25 cores.
- The thermalization time in the QMC solver, which has to be around one fourth of the total QMC time to ensure the system is well equilibrated before measurements are taken.
- The number of imaginary time slices in the QMC solver, which we set to 1024 slices to ensure a good resolution in imaginary time.

To choose appropriate values for n_{DMFT} and t_{QMC}, we examined spectral function plots and monitored the change in quasiparticle weight as these parameters were increased. Playing around with these parameters, we found that increasing both parameters improved convergence at roughly the same rate. Our convergence showed that even very large values of n_{DMFT} and t_{QMC} improved the results (see figure 3), so we set them to the maximum values our time constraints allowed: $t_{\mathrm{QMC}} = 200$ s and $n_{\mathrm{DMFT}} = 200$. You can also see the improvement in the spectral function on figure 4.

The in-house DMFT + QMC code used for this project has two main parameters to ensure convergence: the number of DMFT iterations n_{DMFT} and the time the QMC solver runs for each DMFT iteration, t_{QMC}. Other parameters worth mentioning are:

- The number of cores used for parallelisation, which is bound by the power of the computer used. We set this to 25 cores.

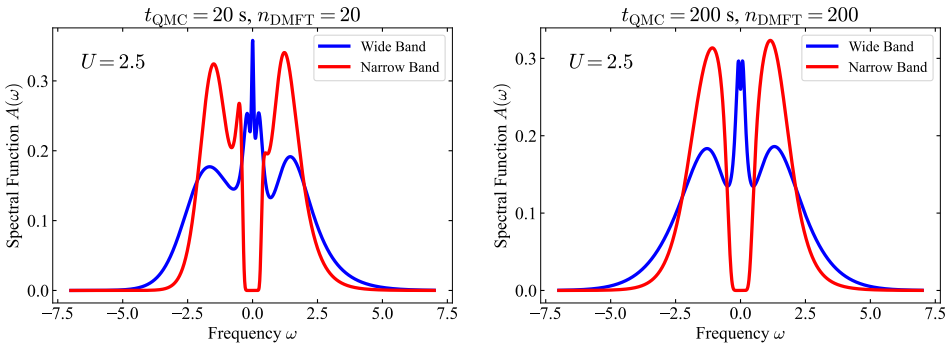

Figure 2: Spectral function for $U = 2.5$ at low (left) and high (right) convergence parameters.

- The thermalization time in the QMC solver, which has to be around one fourth of the total QMC time to ensure the system is well equilibrated before measurements are taken.
- The number of imaginary time slices in the QMC solver, which we set to 1024 slices to ensure a good resolution in imaginary time.

To choose appropriate values for n_{DMFT} and t_{QMC}, we examined spectral function plots and monitored the change in quasiparticle weight as these parameters were increased. Playing around with these parameters, we found that increasing both parameters improved convergence at roughly the same rate. Our convergence showed that even very large values of n_{DMFT} and t_{QMC} improved the results (see figure 3), so we set them to the maximum values our time constraints allowed: $t_{\mathrm{QMC}} = 200$ s and $n_{\mathrm{DMFT}} = 200$. You can also see the improvement in the spectral function on figure 4.

3 Results

The quasiparticle weight is plotted on Fig. **??**. The graph unambiguously shows an OSMT, with the narrow band becoming insulating at $U_{c1} \approx 2.1$ and the wide band at $U_{c2} \approx 3.1$. These results are to be compared with that of Koga's paper [4] and Arita's paper [7], which show respectively $U_{c1} \approx 2.6, U_{c2} \approx 3.5$ and $U_{c1} \approx 2.6$

Overall, our results are lower than those cited above. This might be agreement with theory, predicting that the critical U at which transition occurs goes down as temperature is increased. [9]

In contrast, Knecht et al. [**?**] find lower values in the J_z model, with $U_{c1} \approx 2.1$ and $U_{c2} \approx 2.6$, contradicting Liebsch's finding of the absence of OSMT [3].

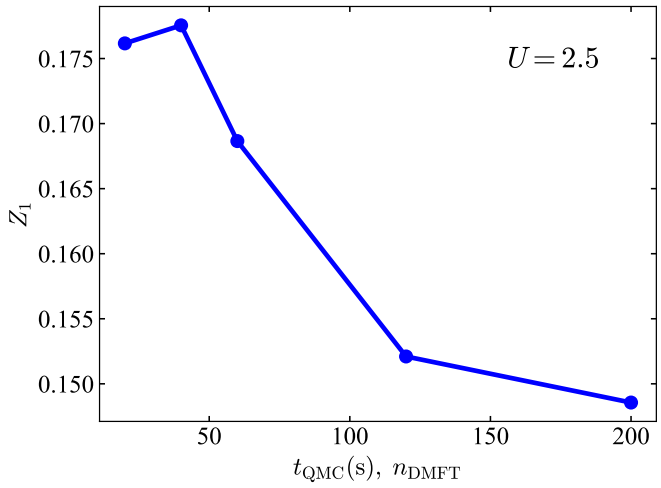

Figure 3: Convergence of the quasiparticle weight as a function of DMFT iterations and QMC time. The number of DMFT iterations and the number of seconds for the QMC time are the same and are varied from 20 to 200.

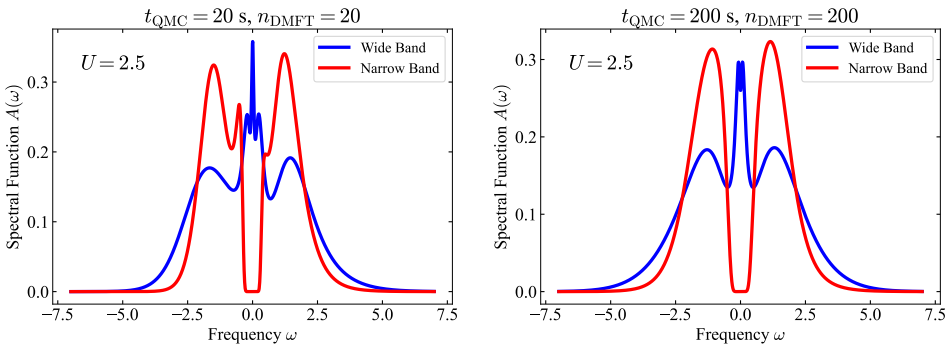

Figure 4: Spectral function for $U = 2.5$ at low (left) and high (right) convergence parameters.

To further ensure our results are correct, we plot the full spectral function for a small set of values of U and assess whether they display the characteristic behaviour of Mott transitions.

We further study the importance of the Hund coupling J by running all the calculations again and setting $J = 0$ this time. The transition value is still not attained at $U = 5.5$, which is the maximum we could attain with our method before convergence issues. The graph seems to be in agreement with Koga's results at $T = 0$ for the same model, where there is a single transition at $U_c = 7.3$, and Z is at about 0.2 for $U = 5.5$.

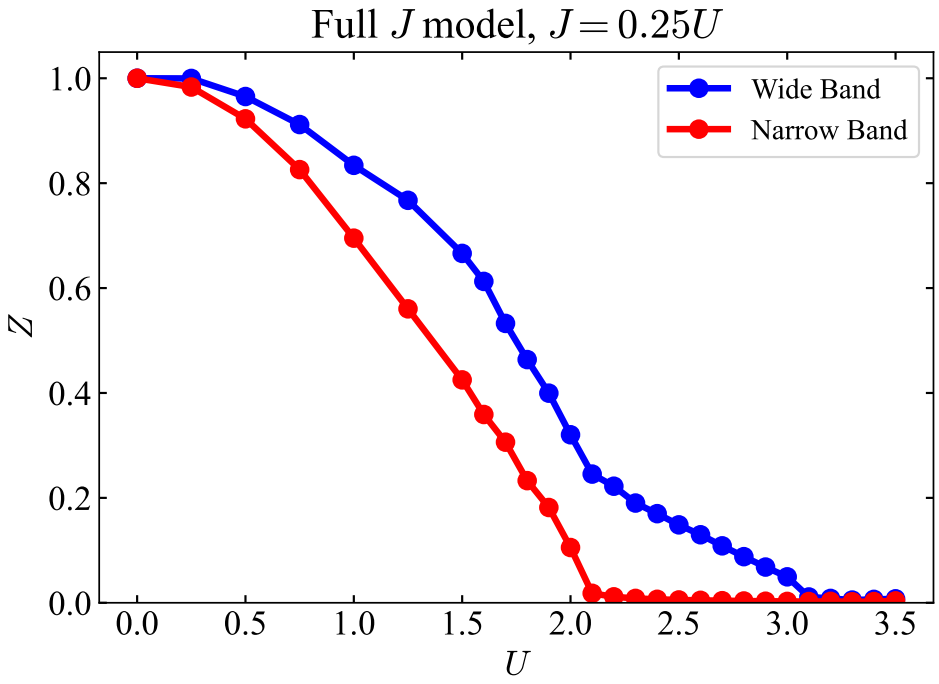

Figure 5: Quasiparticle weight as a function of U for $J = 0.25U$. The critical parameter U_c at which the Mott transition occurs is defined as the point where Z reaches 0.

4 Conclusion

We considered a two-band Hubbard model with two different bandwidths $W_1 = 2\text{eV}$ and $W_2 = 4\text{eV}$ at room temperature $T = 1/40\text{eV}$. The full J model was used, and the interaction strengths fixed at $U' = U/2$ and $J = U/4$. The self energy and the spectral function were calculated using DMFT with a QMC impurity solver. The behaviour of the spectral weight at the Fermi level shows an orbital selective Mott transition. The system undergoes two phase transitions, first at lower U for the narrow band, and at higher U for the wide one. Between the two critical values of U, we obtain an intermediate phase, where the narrow band is insulating and the wide one is still conducting. These findings are in agreement with Knecht et al., who found it for the J_z model at finite temperature, with Koga et al., who found it for the full J model at 0 temperature and Arita and Held, who found it in both models at 0 temperature. In our work, we showed in addition that the transition remains orbital dependent at finite temperature for the full J model (table 1).

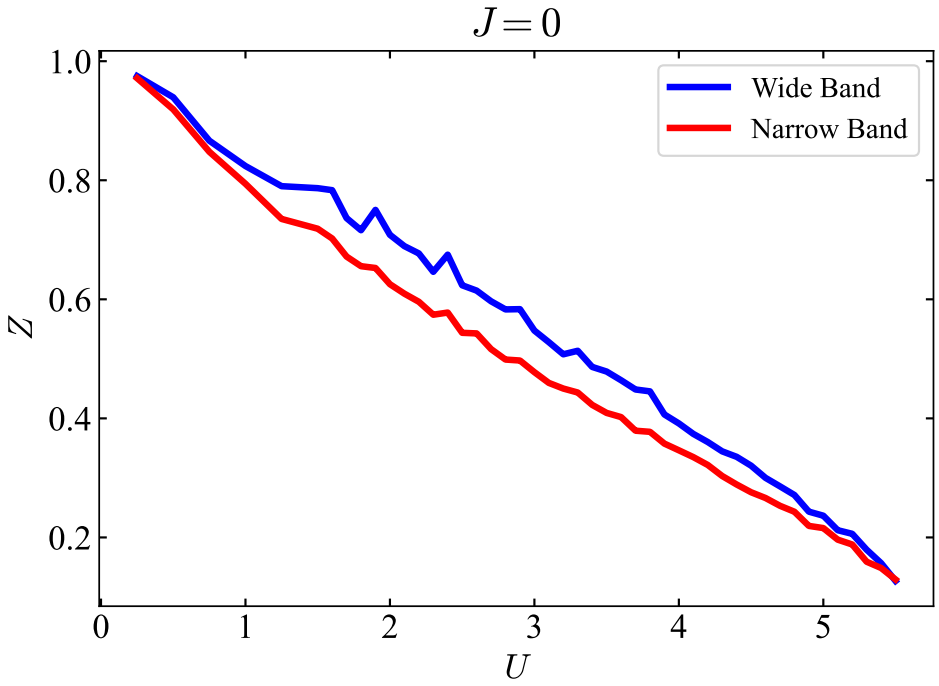

Figure 6: Quasiparticle weight as a function of U for $J = 0$.

		J_z model		J model	
Author	T (eV)	U_{c1} (eV)	U_{c2} (eV)	U_{c1} (eV)	U_{c2} (eV)
Liebsch, 2004	1/32	2.5	2.5		
Koga et al., 2005	0	2.3	2.3	2.6	3.5
Knecht et al., 2005	1/40, 1/32	2.1	2.6		
Arita, Held, 2005	0			2.6	
Our results	1/40			2.1	3.1

Table 1: Table comparing numerical values for Mott transitions. Liebsch's first paper is omitted as the parameters used were too different. Our results are

Acknowledgements

References

[1] S. Nakatsuji and Y. Maeno. Quasi-two-dimensional mott transition system $Ca_{2-x}Sr_xRuO_4$. *Physical Review Letters*, 84(12):2666–2669, March 2000.

[2] A. Liebsch. Mott transitions in multiorbital systems. *Physical Review Letters*, 91(22), November 2003.

[3] A. Liebsch. Single mott transition in the multiorbital hubbard model. *Physical Review B*, 70(16), October 2004.

[4] Akihisa Koga, Norio Kawakami, T. M. Rice, and Manfred Sigrist. Orbital-selective mott transitions in the degenerate hubbard model. *Physical Review Letters*, 92(21), May 2004.

[5] Akihisa Koga, Norio Kawakami, T.M. Rice, and Manfred Sigrist. Mott transitions in the multi-orbital systems. *Physica B: Condensed Matter*, 359–361:1366–1368, April 2005.

[6] C. Knecht, N. Blümer, and P. G. J. van Dongen. Orbital-selective mott transitions in the anisotropic two-band hubbard model at finite temperatures. *Physical Review B*, 72(8), August 2005.

[7] R. Arita and K. Held. Orbital-selective mott-hubbard transition in the two-band hubbard model. *Physical Review B*, 72(20), November 2005.

[8] A. Liebsch. Comment on: "orbital-selective mott transitions in the anisotropic two-band hubbard model at finite temperatures" by c. knecht, n. bluemer, and p. g. j. van dongen, cond-mat/0505106, 2005.

[9] Kensuke Inaba, Akihisa Koga, Sei-ichiro Suga, and Norio Kawakami. Finite-temperature mott transitions in the multiorbital hubbard model. *Physical Review B*, 72(8), August 2005.